Proceedings of the ASME 2016 Fluids Engineering Division Summer Meeting
FEDSM2016
July 10-14, 2016, Washington, DC, USA

FEDSM2016-7768

PARTICLE TRACKING VELOCIMETRY (PTV) MEASUREMENT OF ABRASIVE MICROPARTICLE IMPACT SPEED AND ANGLE IN BOTH AIR-SAND AND SLURRY EROSION TESTERS

Amir Mansouri, Hadi Arabnejad Khanouki, Siamack A. Shirazi, Brenton S. McLaury
Erosion/Corrosion Research Center
Mechanical Engineering Department
The University of Tulsa
800 S Tucker Dr. Tulsa, OK, 74104
Email: amir-mansouri@utulsa.edu

ABSTRACT

Solid particle laden flows are very common in many industries including oil and gas and mining. Repetitive impacts of the solid particles entrained in fluid flow can cause erosion damage in industrial equipment. Among the numerous factors which are known to affect the solid particle erosion rate, the particle impact speed and angle are the most important. It is widely accepted that the erosion rate of material is dependent on the particle speed by a power law V^n, where typically n=2-3. Therefore, accurate measurements of abrasive particle impact speed and angle are very important in solid particle erosion modeling. In this study, utilizing a Particle Image Velocimetry (PIV) system, particle impact conditions were measured in a direct impinging jet geometry. The measurements were conducted with two different test rigs, for both air-sand and liquid-sand flows. In air-sand testing, two types of solid particles, glass beads and sharp sand particles, were used. The measurements in air-sand tests were carried out using particles with various sizes (75, 150, and 500 µm). Also, submerged testing measurements were performed with 300 µm sand particles. In the test conditions, the Stokes number was relatively high (St=3000 for air/sand flow, St=27 for water/sand flow), and abrasive particles were not closely following the fluid streamlines. Therefore, a Particle Tracking Velocimetry (PTV) technique was employed to measure the particle impact speed and its angle with the target surface very near the impact. Furthermore, Computational Fluid Dynamics (CFD) simulations were performed, and the CFD results were compared with the experimental data. It was found that the CFD results are in very good agreement with experimental data.

INTRODUCTION

Solid particle erosion is the gradual removal of material due to repeated impingements of small particles carried by fluid flow. Erosion damage occurs in equipment dealing with gas-solid and liquid-solid mixtures such as pipelines, choke valves, elbows, slurry pumps and slurry mixers in many industrial applications. The cost of erosion in various industries including oil and gas has drawn significant attention among researchers. Mitigation of the erosion severity requires full understanding of the important parameters influencing the erosion rate. Among all of the numerous parameters affecting the erosion rate, particle dynamics (such as particle speed, particle impact angle) are known to have the most significant effect. Accurate measurement of the particle dynamics in erosion testers will aid in the control over the erosion test conditions and ultimately lead to development of accurate erosion models. The main objective of the erosion model is to correlate the particle impingement speed, impact angle and impact frequency with material loss rate for a practical range of conditions.

Many types of erosion testers such as dry impingement jet, centrifugal-accelerator tester, slurry impingement jet, and slurry pot tester are applied by researchers to perform erosive wear studies [1-5]. Also in order to measure the particle velocity, various experimental methodologies such as high-speed photography [6], double-disk velocimeter [7], laser flight-time

velocimeter [8], and laser Doppler anemometry (LDA) [9] were used in the past studies. In the present work, a Particle Image Velocimetry (PIV) system is used to determine the particle dynamics. Also, the PIV system is capable of tracking individual small particles which is called Particle Tracking Velocimetry (PTV) technique. In practical conditions, when erosion damage takes place, the sand particles carrying by fluid flow are larger than seeding particles which are used in PIV measurements. In erosion test conditions the Stokes number is higher than one and as a result the abrasive particles are not closely following the fluid streamlines. Therefore, in the current study the PTV technique was used to track the individual particles.

The previous studies mainly focused on particle velocity measurement in gas-solid erosion testers and no study was found in the literature measuring the particle speed and angle in liquid-solid erosion testers. In the current study using PTV technique, the particle velocity are measured for both gas-solid and liquid-solid erosion testers. The experimental data presented here can be a great aid in predicting the erosion rate in industrial equipment.

GAS-SOLID IMPINGEMENT JET EROSION TESTER

Accurate measurement of the particle impact velocity is essential in determining the erosion rate (*ER*), because it is widely accepted that the eorsion rate is dependent on the particle velocity by a power law V^n [10].

$$ER \propto V^n \tag{1}$$

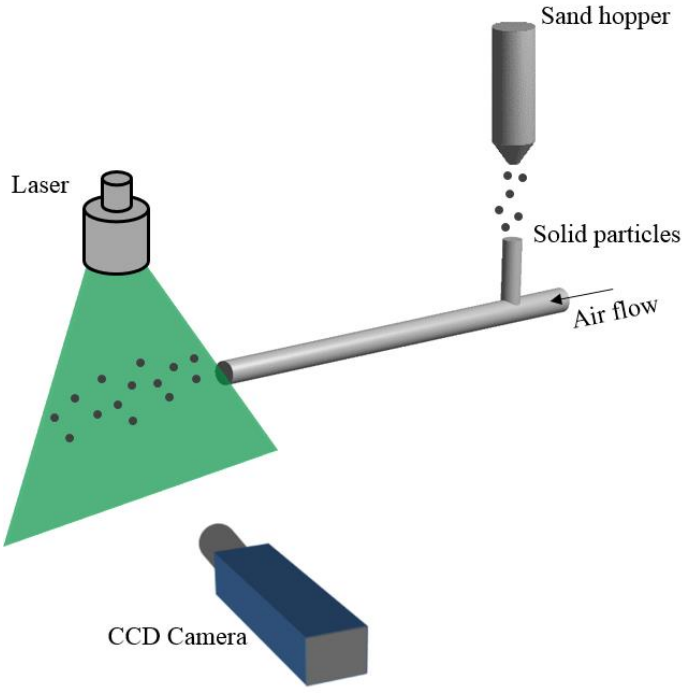

Figure 1. Schematic of the test rig for particle velocity measurement in dry impact erosion tester

In the dry impingement jet erosion tester, particle velocity is controlled by inlet air pressure. As illustrated in Figure 1, the solid particles are mixed with the air flow inside the nozzle. The air flows with high velocity inside the nozzle and draws the solid particles into the nozzle. The high speed gas flow accelarates the microparticles through the drag force. The mixture of gas and solid particles exit from the nozzle and particles impinge the test specimen which is positioned 12.7 mm away from the nozzle exit in erosion tests. However, the test specimen was removed in the particle velocity measurements and particle velocities were measured at 12.7 mm away from the nozzle exit. This approach forces the assumption that the presence of the specimen does not significantly alter the particle impact speed and angle. This assumption is acceptable for relatively large particles at very low concentrations. The test rig consists of a 152.4 mm length nozzle with an internal diameter of 7.6 mm. Two types of particles, sharp sand and rounded glass beads were used. Figures 2 and 3 show Scanning Electron Microscopy (SEM) images of the sand and glass bead particles. In the present work, the particle velocity measurements were performed using a TSI PIV system. The laser source was a pulsed Nd:YAG laser with 200 mJ/pulse output energy and 532 nm wave length. The images were captured by a high resolution (2048×2048 pixel) CCD camera operating with a 100 mm lens. Figure 4 demonstrates the sand particles exiting the jet. The synchronizer with 1 ns resolution automatically controlled the timing between the laser pulses and camera. Traditional PIV calculates the flow field using small seeding particles that follow the streamlines very closely. The PIV technique is limited to flows where the Stokes number (*St*) is less than 0.1. *St* is regarded as the ratio of the particle response time τ_p to the time scale τ_f of the fluid flow:

$$St = \frac{\tau_p}{\tau_f} \tag{2}$$

$$\tau_p = \frac{d_p^2 \rho_p}{18 \mu_f} \tag{3}$$

Where d_p, ρ_p, and μ_f are the particle mean diameter, particle density and fluid viscosity, respectively. In low Stokes number flows, the relative velocity between the particle and the local air velocity is negligible and the traditional PIV technique is applicable. However in order to study the particle dynamics in higher Stokes flows, the PTV technique should be applied. PTV typically captures the microparticles in images with low density of seeded particles. PTV technique accurately locates the individual micro-particles in sparsely seeded images and calculates the particle velocities. To calculate the particle velocities, the postprocessing of the captured images was performed using the software INSIGHT 4G provided by TSI Inc. Figure 5 illustrates the calculated particle velocities exiting from the jet.

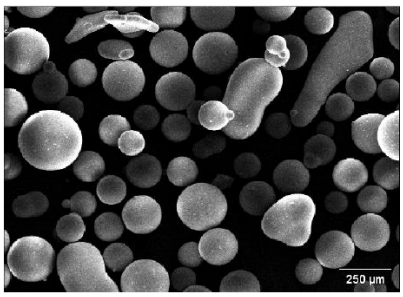

Figure 2. SEM image of the glass bead particles (150 µm)

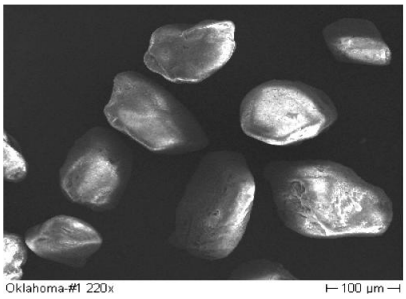

Figure 3. SEM image of the sand particles (150 µm)

In order to obtain a reasonable statistical distribution of the particle velocity, for each test condirtion 100 pairs of images were captured and analyzed. The PTV measurements of the individual particle velocities revealed that for each gas velocity value, there is a wide range of particle velocities. The particle velocity distribution for various gas velocities in the jet (46-112.5 m/s) is demonstrated in Figures 6 and 7. The particle and gas velocities were measured at 12.7 mm away from the jet exit where the test specimen is positioned during the erosion tests. As disscussed earlier, the particle impact velocity has such a significant influence on the erosion rate and it is important to detemine its value with high accuracy. However, the PTV results indicate that the velocity of an individual particle might be different from the mean particle velocity due to variations in particle size, shape, effect of particle-particle interactions, particle-jet wall interactions, and turbulence of the air stream. Since erosion rate is dependent on the particle velocity raised to a power exponenet, any deviation of the particle velocity from the mean value has a strong effect on the predicted erosion rate. Therefore, in addition to mean particle velocity, studying the particle velocity disturbution will be very useful in developing accurate erosion models. The mean particle velocity is compared with the gas velocity (see Figures 8 and 9). Obviously, there is slip between the gas and particle. Particles move with lower speed compared to gas velocity. Furthermore, Figures 8 and 9 show the effect of particle size on the mean particle velocity for the sand and glass bead particles. The smaller particles are accelarated to higher velocities for the same gas velocity. This means that for the same gas velocity flowing in the jet, smaller particles impinge the surface with higher speed and consequently result in higher erosion rates.

Particle shape is another parameter that is affecting the erosion rate. Sharp-edged particles at low impact angles, remove more material from the surface than rounded particles (cutting mechanism). Also, for the same gas velocity flowing in the jet, particle shape can alter the particle velocity. Figures 10 and 11 show that for a given gas velocity, the rounded particles (glass beads) are moving with higher velocities than sharp-edged particles (sand). This can be attributed to the difference of drag forces acting on particles with various shape and angularity. Gas velocity can be correlated to the particle velocity by the following linear equation:

$$V_g = mV_p \tag{4}$$

Where, V_g and V_p are the gas velocity and particle velocity, respectively. The constant m is given in Table 1 for different particles.

Figure 4. Photograph of the sand particles exiting from the jet

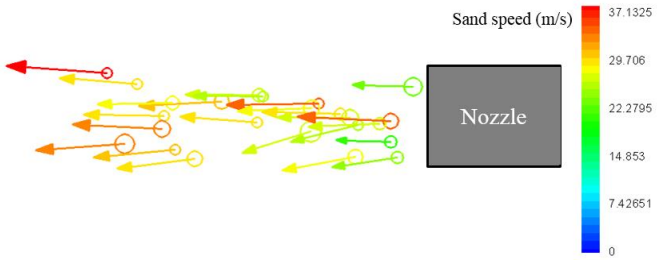

Figure 5. Particle velocities measured by PTV technique

Table 1. *m* values in Eq. 4 for different particles

Particle type	Particle size (µm)	*m*
Glass beads	75	0.520
Glass beads	150	0.396
Glass beads	500	0.283
sand	75	0.415
sand	150	0.312
sand	600	0.170

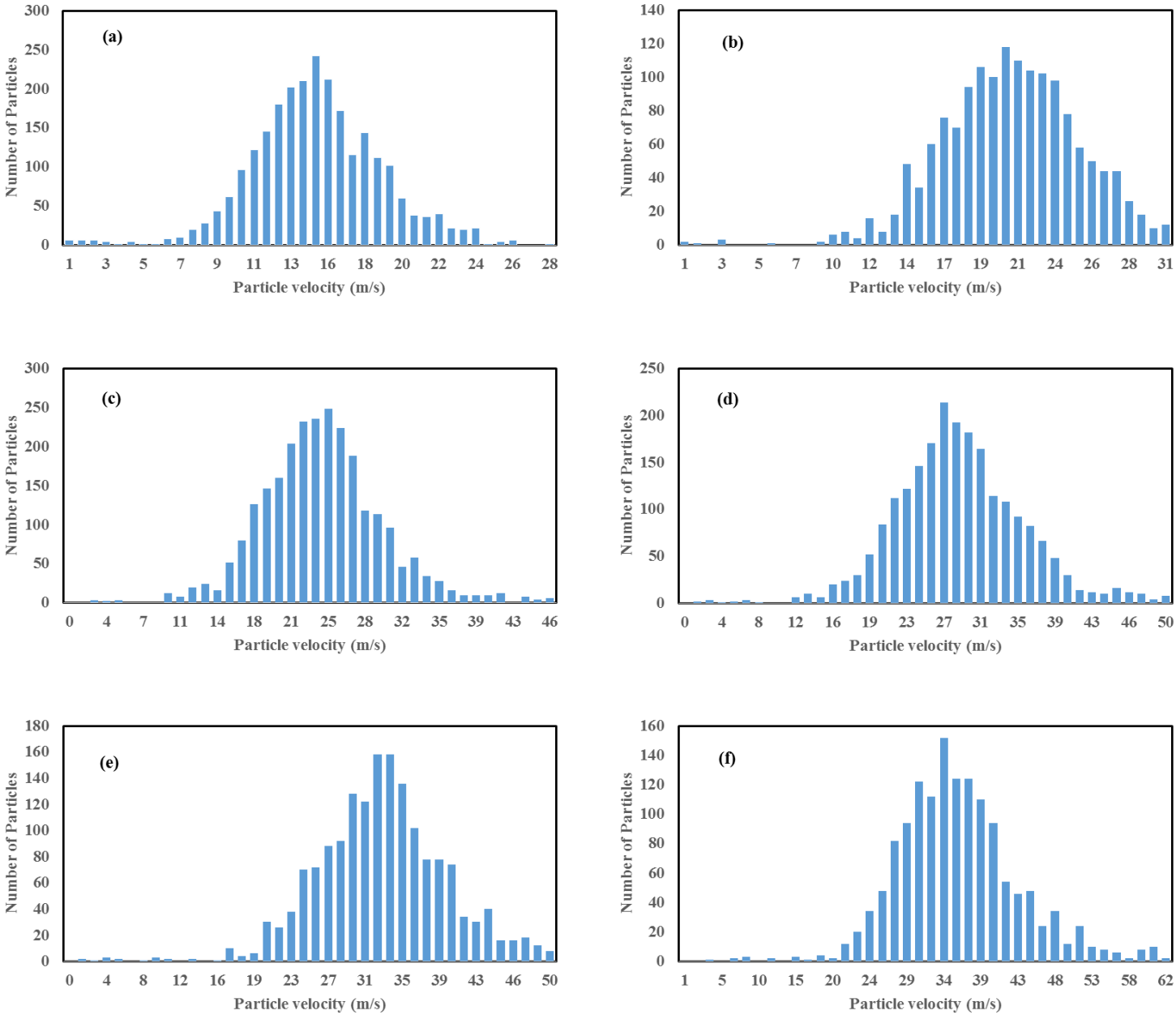

Figure 6. Measured particle velocity distribution for sand particle 150 µm (gas velocity is (a) 46 m/s, (b) 65 m/s, (c) 79.55 m/s, (d) 91.85 m/s, (e) 102.71 m/s, (f) 112.5 m/s)

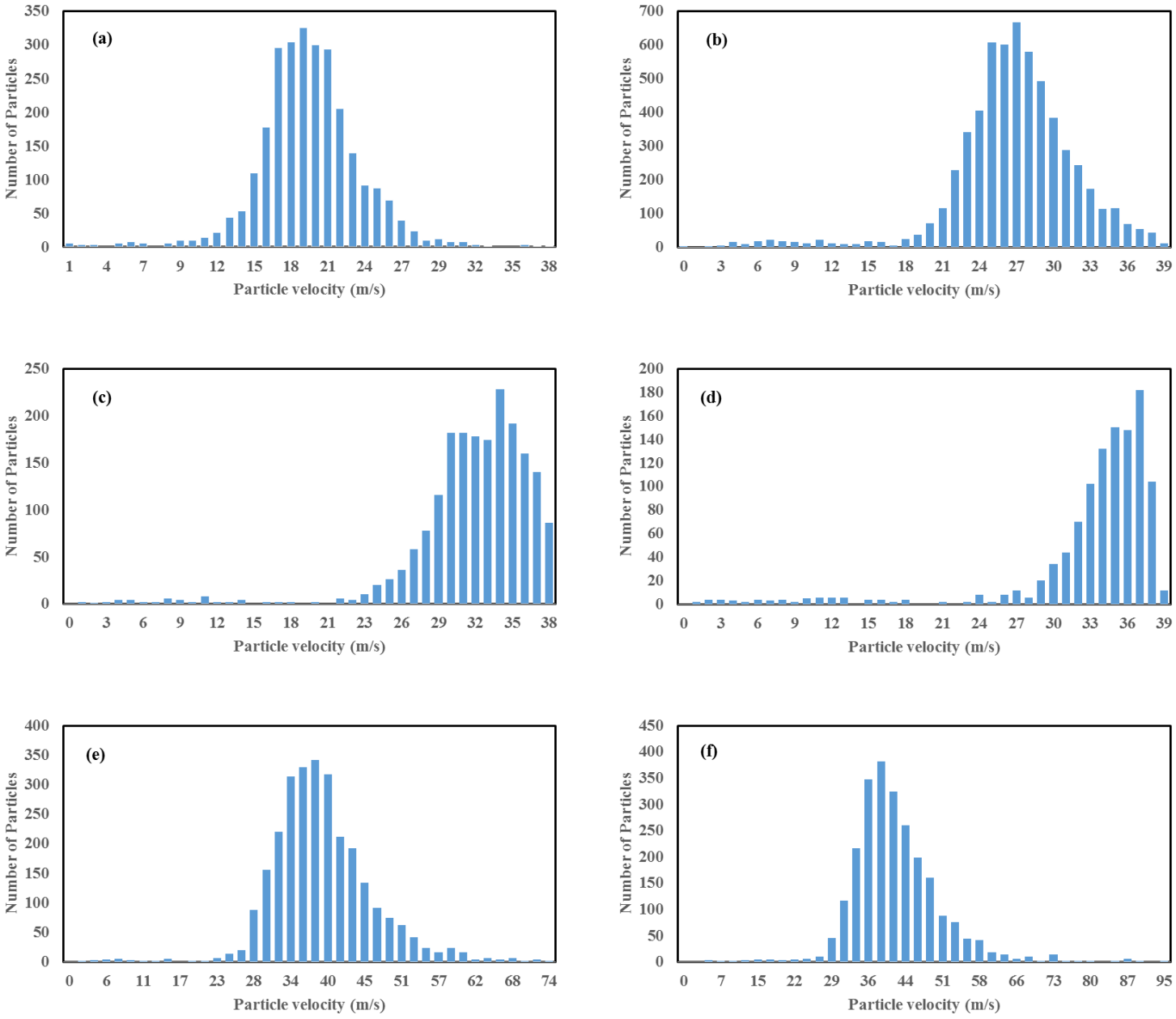

Figure 7. Measured particle velocity distribution for glass beads 150 µm (gas velocity is (a) 46 m/s, (b) 65 m/s, (c) 79.55 m/s, (d) 91.85 m/s, (e) 102.71 m/s, (f) 112.5 m/s)

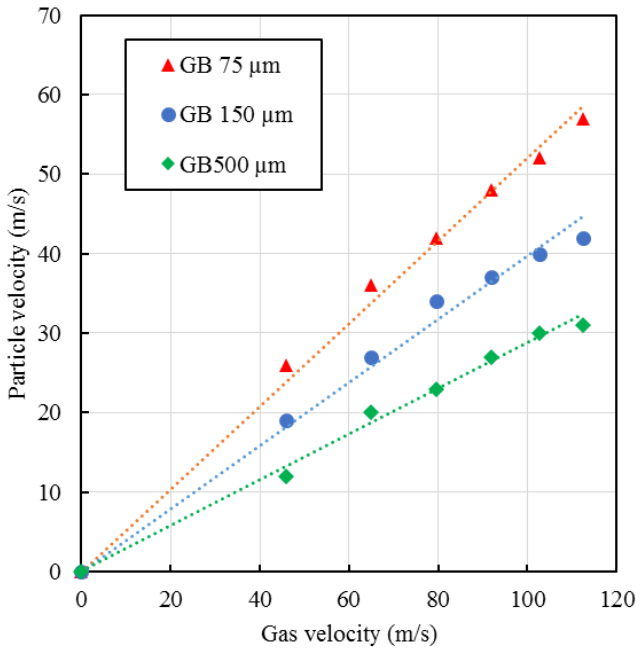

Figure 8. Effect of particle size on the mean particle velocity in gas-solid impinging jet for glass beads (75-500 µm)

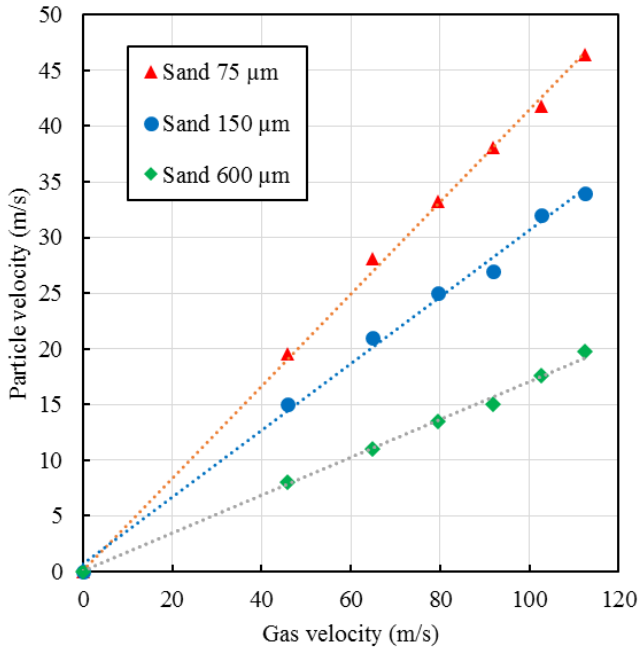

Figure 9. Effect of particle size on the mean particle velocity in gas-solid impinging jet for sand particles (75-600 µm)

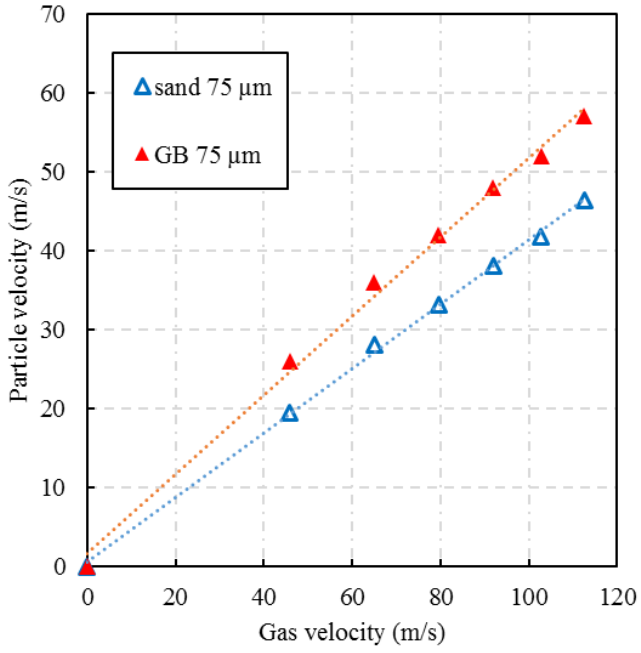

Figure 10. Effect of particle shape on the mean particle velocity in gas-solid impinging jet (75 µm)

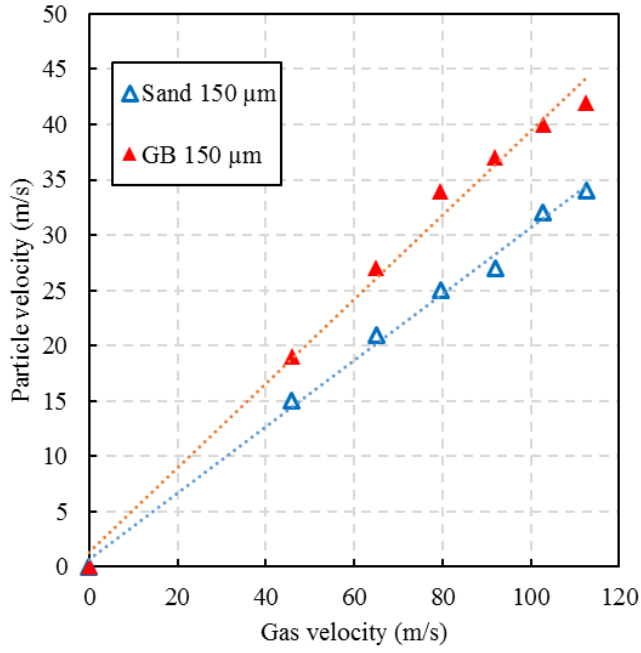

Figure 11. Effect of particle shape on the mean particle velocity in gas-solid impinging jet (150 µm)

LIQUID-SOLID IMPINGEMENT JET EROSION TESTER

The submerged impingement jet erosion tester has been used by many researchers to understand the erosion mechanism occuring in industries dealing with slurry flows. Analyzing the liquid-solid erosion tests is far more complex than gas-solid erosion tests. Previous studies showed that unlike the gas-solid tests, in slurry jet tests the particle impact speeds and angles vary over the target surface [4]. Therefore, it is of great importance to measure the particle speed and angle near the target surface before the particle impinges the surface. Figure 12 illustrates the schematic diagram of the direct impinging jet.

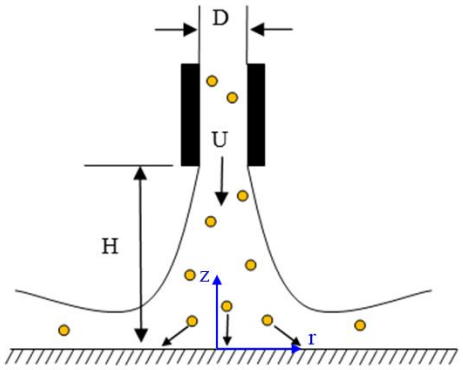

Figure 12. Schematic of the direct impingement jet geometry

As discussed earlier, the PTV technique is a great tool for studying individual particle dynamics. The PTV technique was used to measure the particle impact speed and angle all over the target surface. Figure 13 shows the PIV setup arrangement for measurements in a submerged impinging jet test. The nozzle inner dimater is 7.6 mm, and the stand-off distance between the nozzle exit and target surface is 12.7 mm. The sand-water mixture exits from the jet with an average velocity of U=8.15 m/s. The sand size distribution is shown in Figure 14. The mean sand size was found to be 300 µm.

Images were captured and post processed via PTV technique. Figure 15 shows the particles that were tracked in a sample image. Some of the particles move toward the wall and some are moving away from the wall after rebound. Because rebounding particles do not contribute to material loss, rebounding particles with the positive axial speed were filtered out in the analysis. In order to measure the particle velocities near the wall, the particles approaching the wall within a distance of 0.8 mm of the wall were considered. From 2000 pairs of images, the particle speeds were obtained in the near wall region. The near wall region is divided into small cells with 0.44 mm size in the radial direction. Due to sand size distribution and turbulence of the fluid flow, particle speeds are slightly different in each cell. The average particle speed was calculated in each cell. The average axial and radial components of the particle impact speed at various radial locations near the wall are shown in Figures 16 and 17.

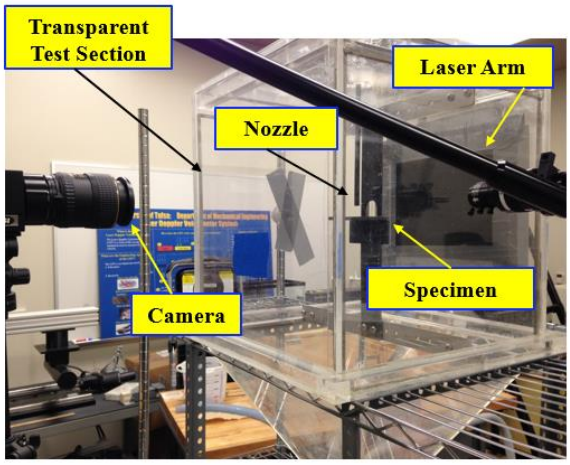

Figure 13. PIV setup arrangement for submerged impingement jet tests

In the erosion process, two mechanisms, deformation and cutting, are known to be important [11]. Deformation mechanism occurs at normal impacts (about 90°), while impacts at low angles cause cutting erosion. Therefore in submerged slurry impinging jet tests, axial and radial components of particle impact speed result in deformation and cutting erosion, respectively. The results in Figure 16 show that at the center of the target surface the axial component is high and as we move further away from the center, the radial component becomes important.

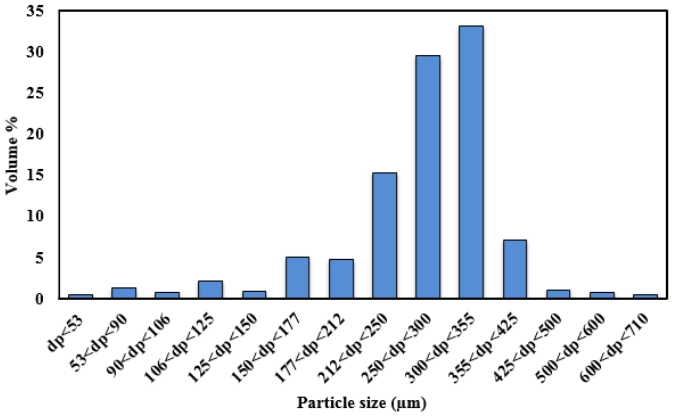

Figure 14. Sand size distribution (mean size 300 µm)

Hence, at the center of the target surface the erosion depth is mainly due to deformation mechanism. At distances away from the center cutting erosion is the dominant mechanism, because the radial component of the particle speed is high. Furthermore, the mean particle impact angle was measured and is shown in Figure 18. The particle impact angle (α) can be calculated using axial and radial velocity components

$$\alpha = \tan^{-1}\left(\frac{V_{axial}}{V_{radial}}\right) \quad (5)$$

The particle impact speed and angle measured in the current work give better insight for developing erosion models, since this information determines how much the deformation and cutting mechanisms contribute to erosion depth at different locations on the target surface.

Also, Computational Fluid Dynamics (CFD) analysis is performed and results are compared with the PTV data. A CFD model for the same test condition was created. The simulations were undertaken with the CFD software ANSYS FLUENT 14.5. The standard k-ε for turbulence model with the scalable wall function was applied. Momentum, turbulent kinetic energy and turbulent dissipation rate equations are discretized by QUICK (Quadratic Upstream Interpolation for Convective Kinematics) scheme. SIMPLE (Semi-Implicit Method for Pressure-Linked Equations) algorithm is employed for treating the pressure–velocity coupling in the equations. A Discrete Particle Method (DPM) model was used for particle tracking and 100,000 particles were released from the jet inlet to obtain a statistically representative particle trajectories. Particle impact speed is influenced by the sand size distribution. Large particles hit the target surface with velocities lower than small particles. Therefore, sand size distribution was considered in CFD modeling using the Rosin-Rammler diameter distribution method. The average particle impact speed and angle were calculated at various radial locations. The CFD results are compared with experimental data in Figures 16, 17, and 18. Very good agreement between the CFD results and PTV measurements was observed.

SUMMARY AND CONCLUSIONS

Particle tracking Velocimetry (PTV) technique was employed to track the micro-particles (sand and glass beads) causing erosion damage. The measurements were conducted in two types of erosion testers (gas-solid and liquid-solid impinging jets). Gas-solid tests show that smaller particles are accelerated to higher velocities for the same gas velocity in the jet. Also for a given air velocity in the jet, spherical particles move faster than angular particles.

The experimental data in slurry tests show that for a fixed nozzle angle (90° in the current study) particles impinge the target surface with a wide range of speeds and angles (0° to 90°). Since particle impact speed and angle are two important parameters affecting the erosion rate, the experimental data presented in this work offers great insight in developing accurate erosion models.

Also, the experimental data obtained from submerged impinging jet tests were compared with CFD results. The CFD data exhibits good agreement with experimental data.

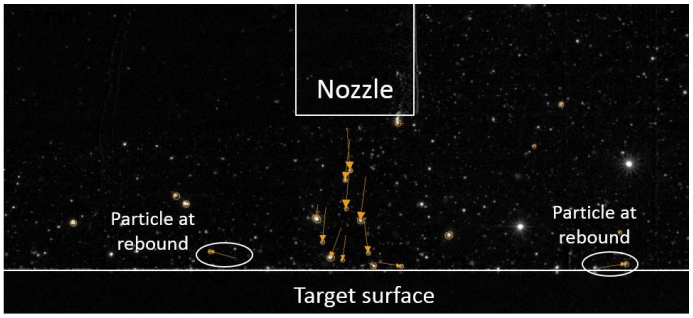

Figure 15. Particle tracking near the wall

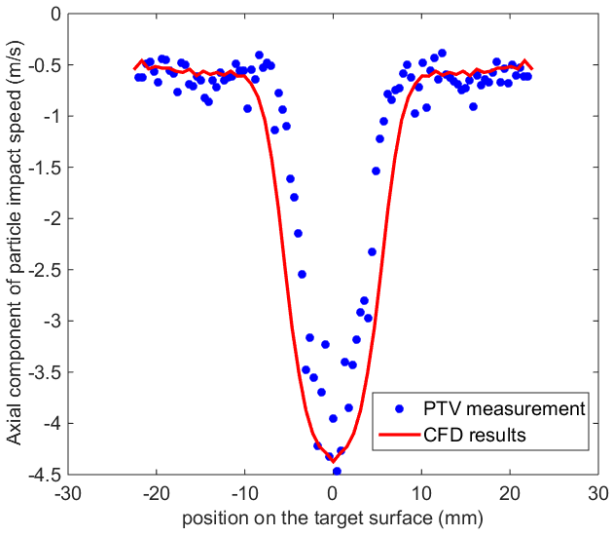

Figure 16. Variation of the axial particle velocity on target surface (sand, mean size 300 µm, *U*=8.15 m/s, *H*=12.7 mm)

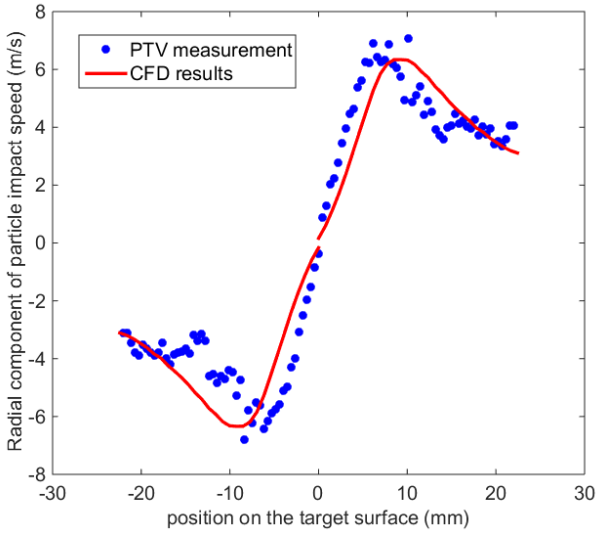

Figure 17. Variation of the radial particle velocity on target surface (sand, mean size 300 µm, *U*=8.15 m/s, *H*=12.7 mm)

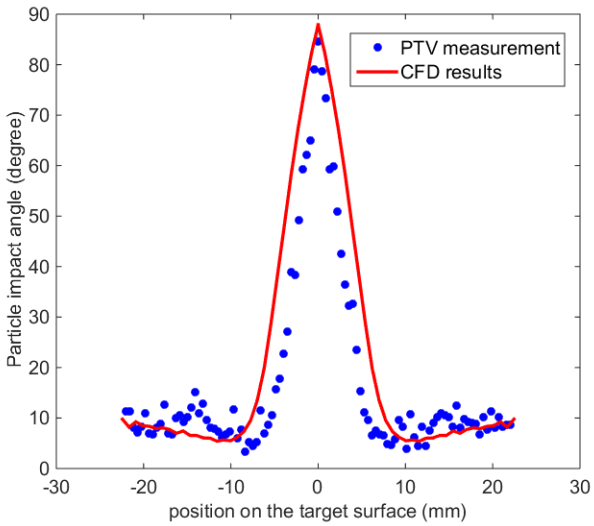

Figure 18. Variation of the particle impact angle on target surface (sand, mean size 300 µm, *U*=8.15 m/s, *H*=12.7 mm)

ACKNOWLEDGMENTS

The authors gratefully acknowledge the financial support by the member companies of Erosion/Corrosion Research Center (E/CRC) at the University of Tulsa. The authors also would like to thank Ed Bowers, senior technician at E/CRC, for his invaluable technical expertise.

REFERENCES

[1] Mansouri, A., Shirazi, S.A. and McLaury, B.S., 2014, Experimental and numerical investigation of the effect of viscosity and particle size on the erosion damage caused by solid particles. ASME 2014 4th Joint US-European Fluids Engineering Division Summer Meeting collocated with the ASME 2014 12th International Conference on Nanochannels, Microchannels, and Minichannels, Paper No. FEDSM2014-21613

[2] Xie, Y., Clark, H.M. and Hawthorne, H.M., 1999. Modelling slurry particle dynamics in the Coriolis erosion tester. Wear, 225, pp.405-416.

[3] Desale, G.R., Gandhi, B.K. and Jain, S.C., 2005. Improvement in the design of a pot tester to simulate erosion wear due to solid–liquid mixture. Wear, 259(1), pp.196-202.

[4] Mansouri, A., Arabnejad, H., Shirazi, S.A. and McLaury, B.S., 2015. A combined CFD/experimental methodology for erosion prediction. Wear, 332-333, pp.1090-1097.

[5] Arabnejad, H., Mansouri, A., Shirazi, S.A. and McLaury, B.S., 2015. Development of mechanistic erosion equation for solid particles. Wear, 332, pp.1044-1050.

[6] Sheldon, G. L., Maji, J. and Crowe, C. T., 1977. Erosion of a tube by gas-particle flow. Journal of Engineering Materials and Technology, 99(2), pp.138-142.

[7] Oka, Y.I., Nishimura, M., Nagahashi, K. and Matsumura, M., 2001. Control and evaluation of particle impact conditions in a sand erosion test facility. Wear, 250(1), pp.736-743.

[8] Kosel, T.H. and Anand, K., 1989. An optoelectronic erodent particle velocimeter. Corrosion and particle erosion at high temperature, The minerals, Metals and Materials Society, pp.349-368.

[9] Deng, T., Bingley, M.S., Bradley, M.S.A. and De Silva, S.R., 2008. A comparison of the gas-blast and centrifugal-accelerator erosion testers: The influence of particle dynamics. Wear, 265(7), pp.945-955.

[10] Finnie, I., 1995. Some reflections on the past and future of erosion. Wear, 186, pp.1-10.

[11] Hutchings, I.M. and Winter, R.E., 1974. Particle erosion of ductile metals: a mechanism of material removal. Wear, 27(1), pp.121-128.